

Upper critical magnetic field of the mixed ternary system $(\text{Sm}_{1-x}\text{Y}_x)\text{Rh}_4\text{B}_4$

S. E. Lambert, J. W. Chen, and M. B. Maple

Department of Physics and Institute for Pure and Applied Physical Sciences, University of California, San Diego, La Jolla, California 92093

(Received 3 July 1984)

The upper critical magnetic field as a function of temperature $H_{c2}(T)$ has been determined for many compositions in the $(\text{Sm}_{1-x}\text{Y}_x)\text{Rh}_4\text{B}_4$ mixed ternary system. For $0 \leq x \leq 0.30$, antiferromagnetic ordering of the Sm^{3+} ions at a temperature T_M enhances H_{c2} above an extrapolation from $T > T_M$. A strong suppression of H_{c2} at low temperature is observed for $0.35 \leq x \leq 0.90$. Calculations of $H_{c2}(T)$ using a multiple-pair-breaking formulation reproduce the trends of the data well, although quantitative agreement is not found for some compositions. This analysis shows that paramagnetic limitation by the uniform component of the exchange field H_J is a very important factor in describing $H_{c2}(T)$ for most compositions. In addition, enhancement of H_{c2} in the antiferromagnetic state due to reductions of spin fluctuations are important for $x \sim 0$.

INTRODUCTION

The interaction of superconductivity with long-range magnetic order has been studied extensively in ternary rare-earth (R) compounds such as RRh_4B_4 , RMO_6S_8 , and RMO_6Se_8 . In particular, the effect of magnetic ordering of R^{3+} ions on the temperature dependence of the upper critical magnetic field $H_{c2}(T)$ has received considerable attention. Of special interest has been the behavior, when antiferromagnetic order occurs, where either enhancement or suppression of $H_{c2}(T)$ has been observed in the various antiferromagnetic superconductors investigated to date.¹ Many theoretical models have been proposed to explain these different types of behavior.¹ In this paper we report the results of an investigation of $H_{c2}(T)$ in the mixed ternary system $(\text{Sm}_{1-x}\text{Y}_x)\text{Rh}_4\text{B}_4$.

The compound SmRh_4B_4 has a superconducting transition temperature T_c of 2.7 K and exhibits the coexistence of superconductivity with long-range antiferromagnetic order below the magnetic ordering temperature $T_M = 0.87$ K,² while YRh_4B_4 has a $T_c = 10.7$ K and is nonmagnetic.³ There were two major motivations for undertaking a study of alloys of these two compounds. First, diluting the antiferromagnetic sublattice of Sm^{3+} ions by substituting nonmagnetic Y for Sm should depress T_M while leaving the superconducting properties relatively unchanged. In particular, we were interested in the dependence on Sm concentration of $H_{c2}(T)$. A second motivation was to provide a reference for comparison with other mixed ternary systems containing Sm. Since Y is trivalent and nonmagnetic, the effects observed here are due solely to the dilution of the Sm^{3+} sublattice.

EXPERIMENTAL DETAILS

Master samples of SmRh_4B_4 and YRh_4B_4 were prepared by arc-melting together stoichiometric amounts of the three elements plus $\sim 4\%$ extra boron by weight to suppress secondary phases.⁴ Samples in the $(\text{Sm}_{1-x}\text{Y}_x)\text{Rh}_4\text{B}_4$ mixed ternary system were prepared by

arc-melting together appropriate amounts of these two master samples, followed by annealing.² Measurements were made of the ac magnetic susceptibility χ_{ac} as a function of temperature in applied magnetic fields H using a four-wire ac bridge operating at 16 Hz. A ^3He - ^4He dilution refrigerator was used to achieve temperatures in the range $0.07 \text{ K} \lesssim T \lesssim 15 \text{ K}$, while magnetic fields were applied with a superconducting solenoid. The temperature was determined from the resistance of two Ge thermometers for $H < 3 \text{ kG}$ ($\sim 1.8 \text{ kG}$ at the location of the thermometers). For $H > 3 \text{ kG}$, a carbon or carbon-glass thermometer was used. The calibration of both carbon thermometers was checked against the Ge thermometers when $H = 0$ after each cool-down. Heat-capacity, C , measurements were made in a semiadiabatic ^3He calorimeter with $H = 0$ to temperatures as low as 0.48 K. The magnetic ordering temperature T_M was defined as the temperature of the maximum in $C(T)$.

RESULTS

Increasing x from 0 in $(\text{Sm}_{1-x}\text{Y}_x)\text{Rh}_4\text{B}_4$ causes a linear decrease of T_M determined from heat capacity with a slope $dT_M/dx = -0.128 \text{ K/at. \% Y}$. An increase of T_c is observed at the same time, with a concentration dependence similar to that observed in $(\text{Sm}_{1-x}\text{Er}_x)\text{Rh}_4\text{B}_4$.⁵ Details of these results will be the subject of a future publication.⁶

Measurements were made of $\chi_{ac}(T, H)$ for bulk samples of all the compositions prepared in this study. Some of these data for $x = 0, 0.20$, and 0.40 are displayed in Figs. 1–3. For all compositions, the transitions are reasonably sharp and well defined, even in applied magnetic fields. A possible complication in interpreting these data is the presence, for some compositions, of superconducting transitions at temperatures higher than the expected T_c . In general, these transitions are considerably broader and exhibit a smaller change in χ_{ac} than the transitions due to the majority of the sample. For these reasons it is easy to distinguish a secondary transition from that due to the

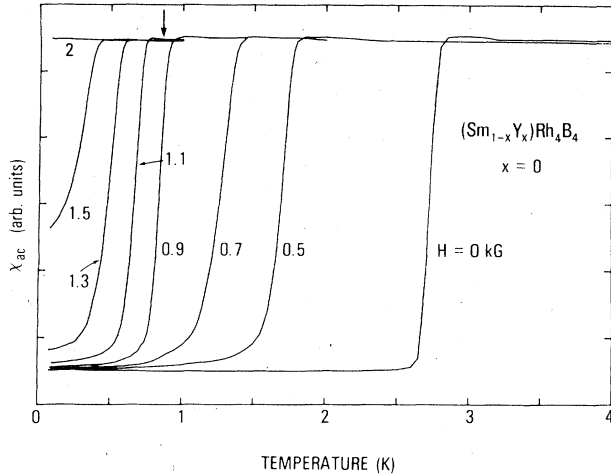


FIG. 1. ac magnetic susceptibility χ_{ac} vs temperature in various applied magnetic fields H indicated in kG, measured for a bulk sample of $(\text{Sm}_{1-x}\text{Y}_x)\text{Rh}_4\text{B}_4$ with $x=0$. The magnetic ordering temperature T_M determined by heat-capacity measurements when $H=0$ is indicated by the arrow. For clarity, data for some magnetic fields are not shown.

phase of interest. There is no indication of these higher-temperature transitions in the $\chi_{ac}(T)$ data for powdered samples from the same ingot, indicating the greater sensitivity of χ_{ac} for bulk samples to the presence of small amounts of impurity phases.

The $\chi_{ac}(T, H)$ data presented in Figs. 1–3 exhibit very different behavior as the composition is varied. For $x=0$, a sharp transition into the superconducting state is observed for each applied field $0 \leq H \leq 1.5$ kG. There is no feature at T_M , except that the transition curves become more closely spaced in temperature for a given increment of applied magnetic field as T decreases below T_M . Note

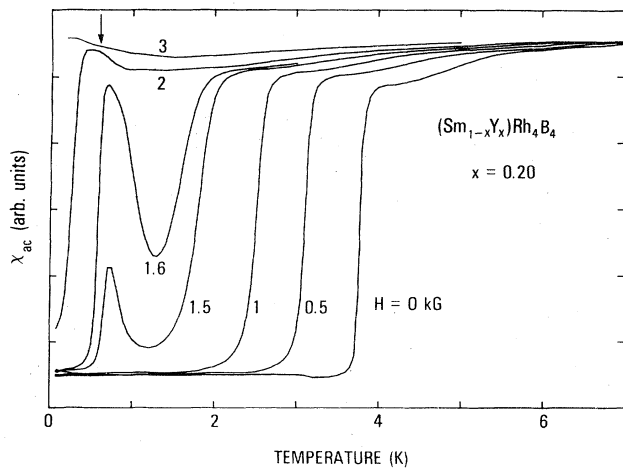


FIG. 2. ac magnetic susceptibility χ_{ac} vs temperature in various applied magnetic fields H indicated in kG, measured for a bulk sample of $(\text{Sm}_{1-x}\text{Y}_x)\text{Rh}_4\text{B}_4$ with $x=0.20$. The magnetic ordering temperature T_M determined by heat-capacity measurements on the same sample when $H=0$ is indicated by the arrow. For clarity, data for some magnetic fields are not shown.

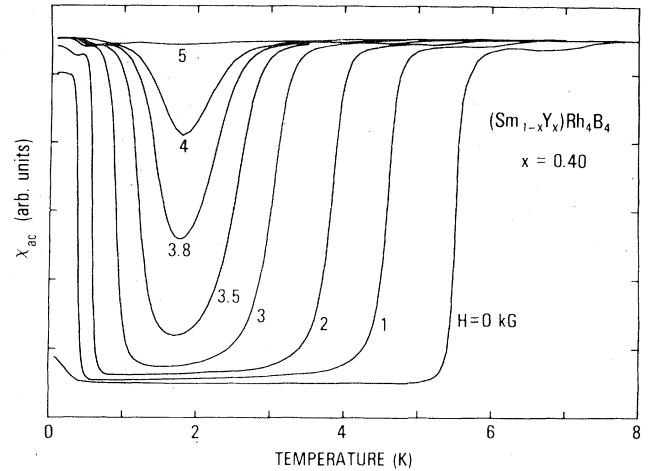


FIG. 3. ac magnetic susceptibility χ_{ac} vs temperature in various applied magnetic fields H indicated in kG, measured for a bulk sample of $(\text{Sm}_{1-x}\text{Y}_x)\text{Rh}_4\text{B}_4$ with $x=0.40$. For clarity, data for some magnetic fields are not shown.

also that there is no peak in $\chi_{ac}(T)$ at T_M for $H=2$ kG, an applied magnetic field for which the sample never becomes superconducting. A small maximum in $\chi_{ac}(T)$ would normally be expected at the antiferromagnetic transition temperature, but relatively small applied magnetic fields can smear out such a feature. Apparently, this occurs in $(\text{Sm}_{1-x}\text{Y}_x)\text{Rh}_4\text{B}_4$ for H as small as 1.5 kG. The data for $x=0.10$ (not shown) are very similar to those for $x=0$.

The data for $x=0.20$ which are displayed in Fig. 2 show very different behavior. For $H=0, 0.5$, and 1 kG, a monotonic decrease of $\chi_{ac}(T)$ is observed as T decreases, with no feature occurring at T_M . For $H=1.5$ and 1.6 kG, a decrease of $\chi_{ac}(T)$ is also observed as the sample becomes superconducting, but the behavior is not the same near T_M . With the temperature decreasing towards T_M , an increase of $\chi_{ac}(T)$ is seen as superconductivity is destroyed in some parts of the sample. This is because the applied magnetic field partially aligns the Sm^{3+} moments, resulting in a magnetization M which should be largest for temperatures just above T_M (assuming H is not large enough to cause a spin-flop or metamagnetic transition). Decreasing the temperature below T_M results in a decrease in M which is favorable for superconductivity, so $\chi_{ac}(T)$ decreases. The result is the prominent peak in $\chi_{ac}(T)$ observed at T_M for $H=1.5$ and 1.6 kG. For larger H , most of the sample is not superconducting above T_M , and a monotonic decrease of $\chi_{ac}(T)$ would be found in the absence of the impurity transitions discussed earlier. The $\chi_{ac}(T, H)$ data for $x=0.20, 0.25$, and 0.30 are all very similar.

The data for $x=0.40$ displayed in Fig. 3 show characteristics very different from the data for smaller x . An increase of $\chi_{ac}(T)$ is found for $T < 1$ K for $H=0$, indicating the partial destruction of superconductivity. No peak is observed in $\chi_{ac}(T)$ at low temperature, which would indicate that superconductivity returns to the sample upon further cooling. More complete destruction of supercon-

ductivity is found as H increases, but there is no decrease of $\chi_{ac}(T)$ at the lowest temperatures. Thus the feature associated with antiferromagnetic ordering for smaller x is absent in the data for $x=0.40$. In fact, the destruction of superconductivity observed for $T \leq 0.4$ K when $H=0$ indicates that at least some of the Sm^{3+} moments exhibit ferromagnetic order for this composition. This is much more obvious in $\chi_{ac}(T)$ data for a powdered sample from the same ingot which show nearly complete destruction of superconductivity for $H=0$. Similar data for powdered samples with $0.30 \leq x \leq 0.50$ show increases in χ_{ac} at low temperature, with the strongest destruction of superconductivity for $x=0.40$. This apparent transition from antiferromagnetic order for $x=0$ to ferromagnetic order for $x \sim 0.4$ will be discussed in more detail in a future publication.⁶

Increasing x further results in $\chi_{ac}(T, H)$ data similar to those for $x=0.40$, except that no destruction of superconductivity is found for $H=0$ down to 80 mK. For sufficiently large magnetic fields, superconducting transitions at high temperatures are followed by increases in $\chi_{ac}(T)$ at lower temperatures which indicate the destruction of superconductivity. As x increases, larger applied magnetic fields are required to destroy superconductivity. However, even for $x=0.90$ (i.e., only 10% Sm^{3+} ions), complete destruction of superconductivity is found at the lowest temperature when $H=16$ kG. For YRh_4B_4 ($x=1$), there are no features indicating destruction of superconductivity at low temperature, as expected for a compound containing no magnetic ions. The data for $x=1$ are very similar to those for $x=0.90$ when $T > 1$ K with comparable transition widths and shapes.

The upper critical magnetic field as a function of temperature $H_{c2}(T)$ can be determined from the $\chi_{ac}(T, H)$ data measured for these $(\text{Sm}_{1-x}\text{Y}_x)\text{Rh}_4\text{B}_4$ samples. The

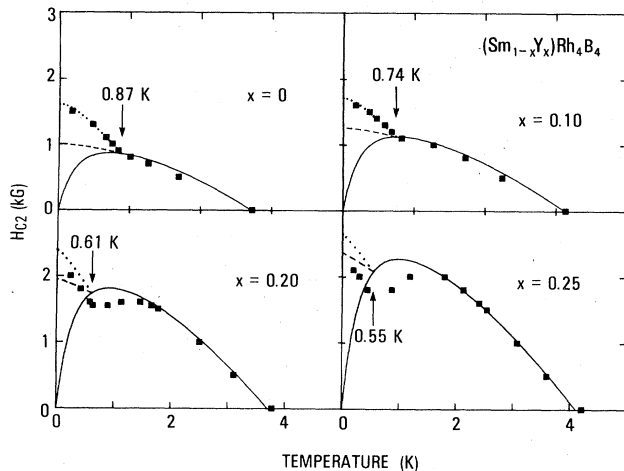


FIG. 4. Upper critical magnetic field H_{c2} vs temperature determined from $\chi_{ac}(T, H)$ measurements for four compositions of $(\text{Sm}_{1-x}\text{Y}_x)\text{Rh}_4\text{B}_4$. Magnetic ordering temperatures T_M determined by heat-capacity measurements on the same sample when $H=0$ are indicated by the arrows. The solid lines are calculations of $H_{c2}(T)$ assuming no magnetic order occurs, while the dashed lines show the influence of antiferromagnetic order at T_M . Dotted lines indicate the effect of a reduction of spin fluctuations in the magnetically ordered state. See text for details.

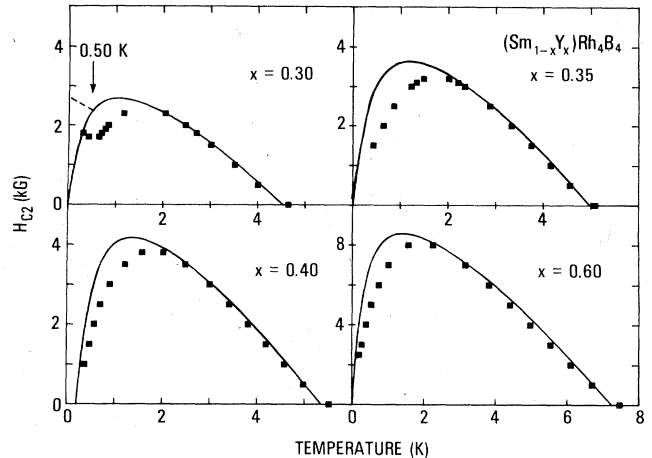


FIG. 5. Upper critical magnetic field H_{c2} vs temperature determined from $\chi_{ac}(T, H)$ measurements for four compositions of $(\text{Sm}_{1-x}\text{Y}_x)\text{Rh}_4\text{B}_4$. The magnetic ordering temperature T_M determined by heat-capacity measurements on the same sample when $H=0$ is indicated by the arrow for $x=0.30$. The solid lines are calculations of $H_{c2}(T)$ assuming no magnetic order occurs, while the dashed line shows the influence of magnetic order at T_M for $x=0.30$. See text for details.

transition temperature for a given H is defined as that temperature where χ_{ac} has the same value as χ_{ac} at the midpoint of the $H=0$ transition. For some samples this is complicated by the presence of the secondary superconducting transitions at higher temperatures mentioned earlier. In these cases, a reasonable estimate is made of the total change due to the larger transition, and the higher-temperature transition is ignored. Because the transitions of interest are sharp, $H_{c2}(T)$ is quite insensitive to the actual value of χ_{ac} chosen as the midpoint of the $H=0$ transition. The $H_{c2}(T)$ curves resulting from this analysis are shown in Figs. 4–6. A previous determination of $H_{c2}(T)$ from ac electrical resistance measurements² for SmRh_4B_4 shows behavior identical to that found here for

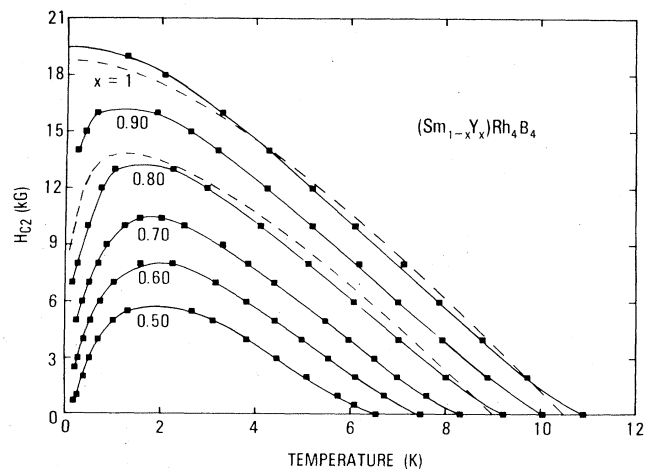


FIG. 6. Upper critical magnetic field H_{c2} vs temperature determined from $\chi_{ac}(T, H)$ measurements for six compositions of $(\text{Sm}_{1-x}\text{Y}_x)\text{Rh}_4\text{B}_4$. Solid lines are guides to the eye. Dashed lines are calculations for $x=0.80$ and 1 using the parameters in Table I. See text for details.

$x=0$, except that the magnitude of the resistively determined H_{c2} is $\sim 13\%$ larger at a given temperature. For $x=0$ and 0.10, an abrupt change occurs in the slope of the $H_{c2}(T)$ curve at T_M , as reflected in the crowding together of the $\chi_{ac}(T)$ transitions for $T < T_M$ mentioned previously. For $x=0.20, 0.25$, and 0.30 , a minimum in $H_{c2}(T)$ is found at T_M which arises from the peaks in $\chi_{ac}(T, H)$ at T_M found for these compositions. The behavior of $H_{c2}(T)$ for $T < T_M$ is similar for these five compositions in that there is an enhancement of $H_{c2}(T)$ above an extrapolation from $T > T_M$.

Only suppression of H_{c2} is observed at low temperature as x increases to 0.35. This strong decrease of H_{c2} at low temperatures results in a bell-shaped $H_{c2}(T)$ curve with a maximum at $H_{\max}=3.2$ kG. The shape of this curve is very similar to that for a ferromagnetic superconductor, except that total destruction of superconductivity is not found at low temperatures for $H=0$. Increasing x results in a uniform increase in H_{\max} to 16.5 kG for $x=0.9$. At the same time, $H_{c2}(T=0)$ increases, although in a less uniform fashion. The result is a family of very similar curves which exhibit a maximum followed by a decrease at lower temperature, as shown in Fig. 6. Finally, for $x=1$ (YRh₄B₄), no suppression of superconductivity is found at low temperature, and a monotonically increasing $H_{c2}(T)$ curve is observed as $T \rightarrow 0$.

ANALYSIS

A theoretical description of these $H_{c2}(T)$ data was made in an attempt to gain insight into the mechanisms that determine $H_{c2}(T)$ in the RRh₄B₄ compounds. The analysis is based on the multiple-pair-breaking theory of Werthamer, Helfand, and Hohenberg,⁷ and Maki,⁸ for a dirty type-II superconductor, modified to include additional pair-breaking effects arising from the presence of magnetic moments.^{9,10} While many expressions for $H_{c2}(T)$ have been proposed to include the influence of magnetic moments,¹ we have used an equation due to Fischer¹⁰ which will be given later. First, a limiting case which is much simpler will be discussed to define the various mechanisms which influence $H_{c2}(T)$.

In the limit of strong spin-orbit (s.o.) scattering, $H_{c2}(T)$ can be expressed as⁹

$$H_{c2}(T) = H_{c2}^*(T) - 4\pi M(H, T) - 3.56H_{c2}^*(0)\lambda_m - 2.15 \times 10^{-5} \frac{\alpha}{\lambda_{s.o.} T_{c0}} [H_{c2}(T) + H_J(M)]^2, \quad (1)$$

where magnetic fields are expressed in gauss. This equation is valid in the dirty limit with spin-orbit scattering infrequent compared to other scattering mechanisms and when

$$\frac{0.281\alpha(H + H_J)}{H_{c2}^*(0)} \left/ \frac{1}{2}(\lambda_{s.o.} - \lambda_m) \right. \ll 1. \quad (2)$$

The orbital critical field $H_{c2}^*(T)$ is the critical field that would be observed in the absence of magnetic moments due to the interaction of H with the momenta of the conduction electrons. The other terms in this expression, which will be discussed below, are due to various mecha-

nisms which act to reduce this orbital critical field to the observed $H_{c2}(T)$.

The $4\pi M(H, T)$ contribution is included since the magnetic field inside the sample is increased by the magnetization M of the Sm³⁺ ions. The next term, $3.56H_{c2}^*(0)\lambda_m$, describes the effect of spin fluctuations of the magnetic moments which suppress superconductivity as described by Abrikosov and Gor'kov.¹¹ The mechanism for this is the exchange interaction between a conduction-electron spin \vec{s} at \vec{r} and a magnetic spin at \vec{R} with total angular momentum \vec{J} , the Hamiltonian for which is¹⁰

$$\mathcal{H} = -2\mathcal{J}(\vec{R} - \vec{r})(g_J - 1)\vec{J} \cdot \vec{s}, \quad (3)$$

where $\mathcal{J}(\vec{R} - \vec{r})$ is a parameter describing the strength and sign of the interaction, and g_J is the Landé g factor. The pair-breaking parameter for uncorrelated magnetic moments is then¹⁰

$$\lambda_m = \frac{cN(0)}{2k_B T_{c0}} (g_J - 1)^2 J(J+1) [\mathcal{J}^2]_{av}, \quad (4)$$

$$[\mathcal{J}^2]_{av} = \frac{1}{2q_F^2} \int_0^{2q_F} q \mathcal{J}^2(q) dq,$$

where the concentration of magnetic moments $c=1$ for pure magnetic material, $N(0)$ is the density of states at the Fermi energy, k_B is Boltzmann's constant, q_F is the Fermi momentum, and $\mathcal{J}(q)$ is the Fourier transform of $\mathcal{J}(|\vec{R} - \vec{r}|)$. Spin fluctuations will be suppressed if magnetic order occurs with an accompanying reduction in λ_m . This will cause an enhancement of $H_{c2}(T)$ as seen from Eq. (1). Several formulations for this effect have been presented¹²⁻¹⁴ which propose various temperature dependences for $\lambda_m(T)$. Another approach is to note that the same equations govern $\lambda_m(T)$ and the reduction in electrical resistance R which can occur when a system of magnetic moments orders magnetically.¹⁵ Such a reduction of R for $T < T_M$ was observed² in normal-state ($H=2$ kG) measurements of SmRh₄B₄. Consequently, the temperature dependence of λ_m for $T < T_M$ is included in this analysis using

$$\lambda_m(T) = \lambda_m(T > T_M) \left[1 - A \frac{\Delta R(T)}{\Delta R(T=0)} \right], \quad (5)$$

where $\Delta R(T)$ is $R(T_M) - R(T)$ for SmRh₄B₄ (Ref. 2) scaled by T/T_M for other compositions in (Sm_{1-x}Y_x)Rh₄B₄. The adjustable parameter A is included since the absolute magnitude of this effect is difficult to calculate. For $A=0$, λ_m remains constant for all temperatures, while for $0 < A \leq 1$, some reduction of λ_m occurs for $T \leq T_M$. The value of A can be reduced from 1 by a variety of effects in the mixed ternary system considered here, including inelastic scattering from spin waves,¹⁵ nonmagnetic effects caused by substituting one rare earth for another,¹⁶ and disorder in the Sm³⁺ sublattice preventing complete suppression of spin fluctuations.

The last term in Eq. (1) describes the paramagnetic limitation of $H_{c2}(T)$ due to disruption of the up-down spin correlation of conduction electrons in the superconducting state by applied or effective magnetic fields. The applied

field $H_{c2}(T)$ can contribute to paramagnetic limitation, but the magnetic fields considered here ($H \lesssim 20$ kG) are too small to have a significant effect. A much more important contribution is from the uniform ($q=0$) component of the exchange field H_J arising from the exchange interaction¹⁰

$$H_J = \frac{2c \mathcal{F}(q=0)(g_J - 1)\langle J \rangle}{g\mu_B}, \quad (6)$$

where $\langle J \rangle$ is the average of J over all the magnetic moments, and μ_B is the Bohr magneton. Since $M \propto \langle J \rangle$, H_J is also proportional to M and is thus equal to zero unless some alignment of the Sm³⁺ moments occurs due to an applied magnetic field or ferromagnetic order. It should be emphasized that H_J is the spatially uniform effective field of Sm³⁺ moments acting upon the conduction-electron spins. No effects due to the spatially varying ($q > 0$) part of the exchange field that occurs in the antiferromagnetic state are included in this analysis. Since $H_J \sim 0.1$ – 1 MG for these materials, a considerable influence of paramagnetic limitation on $H_{c2}(T)$ is possible. The other parameters in this term in Eq. (1) are the Maki parameter $\alpha = 7.69 \times 10^{-5} H_{c2}^*(0)/T_{c0}$, the estimated transition temperature T_{c0} in the absence of magnetic moments when $H=0$, and the spin-orbit scattering parameter $\lambda_{s.o.}$. As can be seen from Eq. (1), the influence of paramagnetic limitation of $H_{c2}(T)$ decreases as $\lambda_{s.o.}$ increases.

The limit given in Eq. (2) is not met at low temperatures for the compounds considered here, and an underestimate would occur if Eq. (1) were used to calculate $H_{c2}(T)$.¹⁷ The more complete expression, which is valid irrespective of the limit given in Eq. (2), is¹⁰

$$\ln(T_{c0}/T) = \left(\frac{1}{2} + ia\right)\psi\left(\frac{1}{2} + \rho_+\right) + \left(\frac{1}{2} - ia\right)\psi\left(\frac{1}{2} + \rho_-\right) - \psi\left(\frac{1}{2}\right), \quad (7)$$

where

$$a = (\lambda_{s.o.} - \lambda_m)/4\gamma,$$

$$\rho_{\pm} = \frac{T_{c0}}{2T} \left[0.281 \frac{H + 4\pi M}{H_{c2}^*(0)} + \lambda_m + \frac{1}{2}(\lambda_{s.o.} - \lambda_m) \pm i\gamma \right],$$

$$\gamma = \left[\left(\frac{0.281\alpha}{H_{c2}^*(0)} (H + H_J) \right)^2 - \frac{1}{4}(\lambda_{s.o.} - \lambda_m)^2 \right]^{1/2},$$

TABLE I. Parameters used to calculate $H_{c2}(T)$ using Eq. (7) for various compositions x of (Sm_{1-x}Y_x)Rh₄B₄. See text for details. For all compositions, $g_J = 0.286$, $J = 2.5$, $\mathcal{F}(q=0) = 0.023$ eV, $T_{c0} = 10.49$ K, and $\lambda_{s.o.} = 0.5$.

x	$H_{c2}^*(0)$ (kG)	H_J (kG)	T_M (K)	Θ (K)	$T_c(H=0)$ (K)	A
0	9	790	0.87	0	2.72	0.082
0.10	9	710	0.75	0	3.13	0.065
0.20	11	630	0.61	0	3.70	0.060
0.25	11.5	590	0.55	0	4.11	0.040
0.30	11.5	550	0.49	0	4.53	0
0.35	13.5	510	0.42	0	4.98	0
0.40	14	470	0.21	0.2	5.35	0
0.60	17	315	0	0	7.26	0
0.80	18.9	160	0	0	9.00	0
1	18.9	0	0	0	10.49	0

and ψ is the digamma function. This equation is valid in the dirty limit when spin-orbit scattering is infrequent compared to other scattering mechanisms.

It is usually assumed that $\mathcal{F}(q)$ in Eq. (4) is independent of q , as in the standard Ruderman-Kittel-Kasuya-Yosida (RKKY) interaction,¹⁸ in which case

$$[\mathcal{F}^2]_{av}^{1/2} = \mathcal{F}(q=0) = \mathcal{F}.$$

A more realistic approximation is $\mathcal{F}(q) = f(q)$, the magnetic form factor of a R^{3+} ion for neutron diffraction¹⁸ which decreases for large q . This is intuitively appealing since in both electron scattering and neutron diffraction it is the spin of the incident particle which interacts with the R^{3+} magnetic moment. Using a calculation of $f(q)$ (Ref. 19) for Sm³⁺ ions and estimating the integral in Eq. (4) results in

$$\mathcal{F}(q=0) = 0.82 [\mathcal{F}^2]_{av}^{1/2},$$

where $E_F = 10.9$ eV has been estimated for SmRh₄B₄ from band-structure calculations for ErRh₄B₄ (Ref. 20) and HoRh₄B₄ (Ref. 21). This calculation of $f(q)$ assumes a spherical Fermi surface and plane waves for the conduction-electron states, neither of which is a good approximation.¹⁸ However, other approximations in the calculation of $H_{c2}(T)$ are probably more important sources of error, and for our purposes, $[\mathcal{F}^2]_{av}^{1/2}$ determined from depression-of- T_c experiments¹⁶ is a reasonable estimate of $\mathcal{F}(q=0)$. Decroux and Fischer comment that

$$\mathcal{F}(q=0) \sim 2[\mathcal{F}^2]_{av}^{1/2}$$

for $R\text{Mo}_6\text{S}_8$ compounds.²²

A very important factor in these calculations is the value of H_J given by Eq. (6). It should be noted that H_J is proportional to $(g_J - 1)J$, not $g_J J$. This means that H_J scales approximately with the square root of the de Gennes factor, $(g_J - 1)[J(J + 1)]^{1/2}$, rather than the saturation moment $g_J J \mu_B$. In particular, H_J for SmRh₄B₄ (790 kG) is actually larger than that for ErRh₄B₄ (660 kG) and TmRh₄B₄ (440 kG), somewhat contrary to intuition since the saturation moment for Sm³⁺ ($0.72\mu_B$) is so much smaller than that for either Er³⁺ ($9\mu_B$) or Tm³⁺ ($7\mu_B$).

The lines in Figs. 4 and 5 and the dashed lines in Fig. 6 are calculations of Eq. (7) using the parameters shown in

Table I. The magnetization was calculated from

$$M(H, T) = \begin{cases} Ng_J \mu_B J B_J(g_J \mu_B J H / k_B (T - \Theta)), & T > T_M \\ \left[\frac{2}{3} + \frac{1}{3} (T/T_M) \right] M(H, T_M), & T \leq T_M \end{cases} \quad (8)$$

where B_J is the Brillouin function, $N = (1-x)9.54 \times 10^{21}$ spins/cm³, $g_J = 0.286$, $J = 2.5$, and $\Theta = 0$ K (except for $x = 0.40$, where $\Theta = 0.2$ K, based on the destruction of superconductivity observed when $H = 0$ for this sample). The magnetic ordering temperature is taken from the linear depression of $T_M(x)$ determined from $C(T)$. The value of $H_J(T=0)$ was calculated from Eq. (6) using $\mathcal{J}(q=0) \sim [\mathcal{J}_{\text{av}}^2]^{1/2} = 0.023$ eV,¹⁶ yielding 790 kG for SmRh₄B₄. The dependence on composition, field, and temperature are included as

$$H_J(T, H) = 790 \text{ kG} (1-x) B_J(g_J \mu_B J H / k_B (T - \Theta)). \quad (9)$$

An extrapolation of the linear portion of $H_{c2}(T)$ to $H = 0$ gives $T_c(H=0)$, while λ_m has the value necessary to depress the $H = 0$ transition temperature from T_{c0} to $T_c(H=0)$, where $T_{c0} = 10.49$ K = $T_c(H=0)$ for YRh₄B₄.

The parameters in the preceding paragraph are all fixed by experimental data or theoretical calculation without considering the experimental results for $H_{c2}(T)$. This leaves only two quantities which can be varied for $T > T_M$ to give agreement with the data: $\lambda_{s.o.}$ and $H_{c2}^*(0)$. The values for $H_{c2}^*(0)$ shown in Table I were chosen to give reasonable agreement with the initial increase of $H_{c2}(T)$ from $H = 0$. The value $\lambda_{s.o.} = 0.5$ was chosen for good agreement with the $x = 0.80$ data near $T = 0$, where the detailed behavior of $M(H, T)$ should be less important. This value of $\lambda_{s.o.}$ was assumed for all other x . Finally, for $T < T_M$, a temperature-dependent reduction of λ_m scaled by the parameter A in Eq. (5) was required to match the observed enhancement of $H_{c2}(T)$ for $0 \leq x \leq 0.25$.

Several ways that magnetic order of the R^{3+} magnetic moments can influence $H_{c2}(T)$ for RRh_4B_4 compounds are illustrated in Figs. 4 and 5. First, assume that no magnetic order occurs, so that the Sm^{3+} moments are saturated as $T \rightarrow 0$, i.e., $T_M = 0$ in Eq. (8). This results in very strong suppression of $H_{c2}(T)$ at low temperature, as shown by the solid lines in Figs. 4 and 5, due to the $4\pi M$ term in Eq. (7) and the influence of paramagnetic limitation by H_J . This strong decrease is not observed for $T < T_M$ in the data for $0 \leq x \leq 0.30$. This can be explained by reductions in H_J and M which begin at T_M due to the antiferromagnetic ordering of the Sm^{3+} moments. The resulting enhancement of H_{c2} is shown by the dashed lines. This calculation does not reproduce the qualitative behavior of the data points for $0 \leq x \leq 0.25$, so the reduction of λ_m according to Eq. (5) is included, as shown by the dotted lines. For $x = 0$ and 0.10, the enhancement of $H_{c2}(T < T_M)$ above an extrapolation from $T > T_M$ is seen to be due almost entirely to a reduction of spin fluctuations and a consequent decrease in λ_m .

No increase of $H_{c2}(T)$ is found at low temperature for $x \geq 0.40$, indicating that antiferromagnetic order does not occur for this range of compositions. Instead, a strong suppression of $H_{c2}(T)$ is found since the Sm^{3+} moments are saturated at low temperature. Calculations are shown

for $x = 0.40$ and 0.60 by solid lines in Fig. 5, and by dashed lines for $x = 0.80$ and 1 in Fig. 6. The data points in Fig. 6 are connected by solid lines as guides to the eye.

There is always the possibility that the $H_{c2}(T)$ curves observed in the $(Sm_{1-x}Y_x)Rh_4B_4$ mixed ternary system are due to some peculiar property of YRh₄B₄. In order to investigate this possibility, a sample of $(Sm_{0.5}Lu_{0.5})Rh_4B_4$ was synthesized since Lu is a nonmagnetic rare earth like Y. The behavior of $H_{c2}(T)$ for this sample and for $(Sm_{0.5}Y_{0.5})Rh_4B_4$ is identical except for the maximum value of $H_{c2}(T)$, which is slightly higher for the Lu compound, consistent with the higher T_{c0} . This shows that the behavior observed for $(Sm_{1-x}Y_x)Rh_4B_4$ is an inherent property of SmRh₄B₄ resulting from dilution of the Sm^{3+} sublattice.

DISCUSSION

The calculations presented here permit a systematic description of the behavior of $H_{c2}(T)$ for the $(Sm_{1-x}Y_x)Rh_4B_4$ mixed ternary system. Considering the data and calculated curves in Fig. 4–6, a strong suppression of $H_{c2}(T)$ at low temperature would be observed in the absence of magnetic ordering for all $x < 0.9$ due to the $4\pi M$ and H_J terms in Eq. (7). This suppression is interrupted at T_M for $0 \leq x \leq 0.30$ when antiferromagnetic ordering occurs. The reduction of M and H_J as the temperature decreases below T_M can result in considerable enhancement of H_{c2} above a calculation, assuming no magnetic order occurs. Reduction of spin fluctuations according to Eq. (5) results in further enhancement of H_{c2} . These calculated curves show excellent qualitative agreement with the data points. All of the trends in the data are reproduced, including the development of a maximum in H_{c2} as x increases from 0. It should be noted that only one parameter [$H_{c2}^*(0)$] was varied freely as a function of x for $T > T_M$. The other adjustable parameter, A , in Eq. (5), decreases as Y is substituted for Sm. This may indicate that disorder in the Sm^{3+} sublattice lessens the effect of magnetic order on spin fluctuations.

Quantitative agreement of the calculations with the data is not as good. When $H_{c2}(T)$ exhibits a maximum, the theoretical curve overestimates the value of H_{c2} . A major contribution to this error is $M(H, T)$ calculated using Eq. (8). For a system which exhibits magnetic order, $\Theta = 0$ is not a reasonable assumption. In particular, the transition from antiferromagnetism to ferromagnetism postulated for $x \sim 0.4$ will, in principle, cause Θ to change from negative to positive. Deviations from B_J behavior are also likely close to T_M , the most crucial region. Furthermore, SmRh₄B₄ is probably not a simple antiferromagnet since both NdRh₄B₄ (Ref. 23) and TmRh₄B₄ (Ref. 24) show sinusoidally modulated magnetic structures. If this is also the case for SmRh₄B₄, then $M(H, T)$ as given by Eq. (8) is, at best, an approximation of the actual behavior. A more detailed analysis using empirically determined crystal-field parameters²⁵ to calculate $M(H, T)$ would help to remove this uncertainty, although it would be very difficult for $T < T_M$. These considerations suggest that quantitative agreement between theory and experiment would be best attained with measured

$M(H, T)$. Even in this case, however, anisotropy of the magnetic properties of RRh₄B₄ compounds could make realistic calculations difficult for polycrystalline samples. A sample in which crystallites have random orientations could exhibit an inhomogeneous state in which strongly magnetized crystallites which are not superconducting contribute to average values of $M(H, T)$ considerably larger than $M(H, T)$ in the superconducting crystallites. Experiments are planned to measure $M(H, T)$ to $T \sim 0.4$ K to test these ideas. Measurements of χ_{dc} in $H = 4.3$ kG have been performed previously for SmRh₄B₄ to $T = 0.71$ K.² However, the influence of M and H_J on H_{c2} for SmRh₄B₄ as shown in Fig. 4 is sufficiently small that using these measured data results in no significant difference in the calculated curve. A smaller source of error in these $H_{c2}(T)$ calculations is the discrepancy observed between the experimental and calculated $H_{c2}(T)$ for YRh₄B₄, where no contributions due to M occur. A correction could be applied to Eq. (7) to account for this.

The measurements and calculations discussed above provide a natural explanation for one puzzle in magnetic superconductors. The compound SmRh₄B₄ is unique among the antiferromagnetic superconductors discovered to date in that $H_{c2}(T)$ increases monotonically as the temperature decreases, while a minimum is found at T_M in other such materials.¹ It is clear from the solid line in Fig. 4 for $x = 0$ that, if the antiferromagnetic ordering temperature were lower, SmRh₄B₄ would also exhibit a minimum at T_M since contributions by M and H_J would have caused $H_{c2}(T)$ to achieve a maximum and begin to decrease for $T > T_M$. Consequently, the absence of a minimum in $H_{c2}(T)$ at T_M for SmRh₄B₄ is the result of the small values of $M(H, T_M)$. This behavior is not surprising in retrospect. The temperature dependence of H_J and M scales with the Brillouin function B_J , the argument of which is $g_J J \mu_B H / k_B (T - \Theta)$. The value of $g_J J$ for Sm³⁺ ions is 0.72, a factor of at least 4.5 lower than any other magnetic R³⁺ ion for which RRh₄B₄ is an antiferromagnetic superconductor. This means that the temperature must be at least 4.5 times lower for similar values of B_J to occur, assuming comparable values for Θ and H . This argument also applies to Chevrel-phase compounds. Should SmMo₆S₈ or SmMo₆Se₈ be shown to exhibit the coexistence of superconductivity and antiferromagnetism, an $H_{c2}(T)$ curve like that of SmRh₄B₄ is expected if T_M is not too low.

Another observation can be made that is based on the behavior of $H_{c2}(T)$ for $x = 0.90$, which is suppressed by ~ 4 kG at $T = 0$ even though the Sm³⁺ sublattice is strongly diluted by Y in this case. The maximum value of

$4\pi M$ is 80 G, and long-range magnetic order is unlikely when only 10% of the R³⁺ ions carry localized magnetic moments. This means that paramagnetic limitation of H_{c2} by H_J is the only mechanism discussed here which can account for the observed behavior. This strong suppression of superconductivity at low temperature observed for $x = 0.90$ shows that even essentially noninteracting Sm³⁺ spins can strongly influence $H_{c2}(T)$.

Finally, only enhancement of $H_{c2}(T)$ is found for $T < T_M$ when magnetic order and superconductivity coexist in the (Sm_{1-x}Y_x)Rh₄B₄ mixed ternary system. This indicates that the additional pair-breaking mechanisms for antiferromagnetic superconductors proposed by various authors¹ are not important in these compounds. In particular, one calculation¹² reveals that the pair-breaking effect of the spatially varying exchange field H_Q which opens a gap in the Fermi surface is decreased by disorder in the R³⁺ sublattice. This result is not applicable to the (Sm_{1-x}Y_x)Rh₄B₄ system since no additional pair breaking attributable to H_Q is observed when $T \leq T_M$, even when $x = 0$.

CONCLUSIONS

Data for $H_{c2}(T)$ have been presented for many compositions in the (Sm_{1-x}Y_x)Rh₄B₄ mixed ternary system. Antiferromagnetic order is indicated for $0 \leq x \leq 0.30$ by enhancement of H_{c2} for ($T < T_M$) above an extrapolation from $T > T_M$. For $0.35 \leq x < 1$, a strong suppression of $H_{c2}(T)$ is found at low temperature. Calculations of $H_{c2}(T)$ using a multiple-pair-breaking formulation¹⁰ reproduce the trends in the data, although quantitative agreement may require measured values of the magnetization near T_M . These calculations show that the monotonic increase of H_{c2} as the temperature decreases for SmRh₄B₄ is due to the small values of M and H_J at T_M . The enhancement of $H_{c2}(T)$ observed for $T < T_M$ in SmRh₄B₄ is well described as a reduction in the Abrikosov-Gor'kov pair-breaking mechanism due to a decrease in spin fluctuations. In addition, suppression of $H_{c2}(T)$ by ~ 4 kG for $x = 0.90$ is evidence for the importance of paramagnetic limitation by the uniform exchange field H_J .

ACKNOWLEDGMENTS

We are grateful to M. Decroux for many helpful discussions. This research was supported by the U.S. Department of Energy under Contract No. DE-AT03-76ER70227.

¹Reviews of recent work can be found in *Topics in Current Physics*, edited by M. B. Maple and Ø. Fischer (Springer, New York, 1982), Vol. 34.

²H. C. Hamaker, L. D. Woolf, H. B. MacKay, Z. Fisk, and M. B. Maple, *Solid State Commun.* **32**, 289 (1979).

³B. T. Matthias, E. Corenzwit, J. M. Vandenberg, and H. Barz, *Proc. Nat. Acad. Sci. U.S.A.* **74**, 1334 (1977).

⁴D. C. Johnston and H. F. Braun, in *Topics in Current Physics*, edited by Ø. Fischer and M. B. Maple (Springer, New York, 1982), Vol. 32, p. 111.

⁵L. D. Woolf and M. B. Maple, in *Ternary Superconductors*, edited by G. K. Shenoy, B. D. Dunlap, and F. Y. Fradin (North-Holland, New York, 1981), p. 181.

⁶S. E. Lambert and M. B. Maple (unpublished).

- ⁷N. R. Werthamer, E. Helfand, and P. C. Hohenberg, *Phys. Rev.* **147**, 259 (1966).
- ⁸K. Maki, *Physics* **1**, 21 (1964).
- ⁹Ø. Fischer, M. Ishikawa, M. Pelizzone, and A. Treyvaud, *J. Phys. (Paris) Colloq.* **40**, C5-89 (1979).
- ¹⁰Ø. Fischer, *Helv. Phys. Acta* **45**, 331 (1972).
- ¹¹A. A. Abrikosov and L. P. Gor'kov, *Zh. Eksp. Teor. Fiz.* **39**, 1781 (1960) [*Sov. Phys.—JETP* **12**, 1243 (1961)].
- ¹²C. Ro and K. Levin, *Phys. Rev. B* **29**, 6155 (1984).
- ¹³K. H. Bennemann, J. W. Garland, and F. M. Mueller, *Phys. Rev. Lett.* **23**, 169 (1969).
- ¹⁴K. Machida, *J. Low Temp. Phys.* **37**, 583 (1979).
- ¹⁵T. V. Ramakrishnan and C. M. Varma, *Phys. Rev. B* **24**, 137 (1981).
- ¹⁶H. B. MacKay, L. D. Woolf, M. B. Maple, and D. C. Johnston, *J. Low Temp. Phys.* **41**, 639 (1980).
- ¹⁷S. E. Lambert, Ph.D. thesis, University of California, San Diego, 1983.
- ¹⁸B. N. Harmon and A. J. Freeman, *Phys. Rev. B* **10**, 4849 (1974).
- ¹⁹C. Stassis, H. W. Deckman, B. N. Harmon, J. P. Desclaux, and A. J. Freeman, *Phys. Rev. B* **15**, 369 (1977).
- ²⁰T. Jarlborg, A. J. Freeman, and T. J. Watson-Yang, *Phys. Rev. Lett.* **39**, 1032 (1977).
- ²¹A. J. Freeman and T. Jarlborg, *J. Appl. Phys.* **50**, 1876 (1979).
- ²²M. Decroux and Ø. Fischer, in *Topics in Current Physics*, Ref. 1, Vol. 34, p. 57.
- ²³C. F. Majkrzak, D. E. Cox, G. Shirane, H. A. Mook, H. C. Hamaker, H. B. MacKay, Z. Fisk, and M. B. Maple, *Phys. Rev. B* **26**, 245 (1982).
- ²⁴C. F. Majkrzak, S. K. Satija, G. Shirane, H. C. Hamaker, Z. Fisk, and M. B. Maple, *Phys. Rev. B* **27**, 2889 (1983).
- ²⁵B. D. Dunlap, L. N. Hall, F. Behroozi, G. W. Crabtree, and D. G. Niarchos, *Phys. Rev. B* **29**, 6244 (1984).